Differential remodelling of peroxisome function underpins the environmental and metabolic adaptability of diplonemids and kinetoplastids

Jorge Morales, Muneaki Hashimoto, Tom A. Williams, Hiroko Hirawake-Mogi, Takashi Makiuchi, Akiko Tsubouchi, Naoko Kaga, Hikari Taka, Tsutomu Fujimura, Masato Koike, Toshihiro Mita, Frédéric Bringaud, Juan L. Concepción, Tetsuo Hashimoto, T. Martin Embley and Takeshi Nara

Supplementary material

Supplementary materials and methods

(a) Enzyme activity

Cells of the mid-log phase were collected, washed twice with 10% (v/v) mannitol and resuspended in 50 mM Tris-HCl/2 mM EDTA pH 7 with protease inhibitor cocktail (Complete, Mini, Roche Diagnostics K.K., Tokyo, Japan). Cells were disrupted by sonication, centrifuged at 26,000 x *g* for 20 minutes, and the supernatant was used to measure the enzymatic activity described as follows; hexokinase and glucokinase [1], phosphoglucose isomerase [2], phosphofructokinase [3], fructose-1,6-biphosphate aldolase [4], GAPDH [5], triose-phosphate isomerase [6], phosphoglycerate kinase [7], phosphoglycerate mutase [8], enolase [9], pyruvate kinase [10], and fructose-1,6-biphosphatase [11].

(b) Antibodies

The mouse antiserum to *D. papillatum* FBPA was produced as described [12]. To obtain antisera to glycolytic enzymes, the cDNA clones of interest were obtained by PCR, cloned in pET151/D-TOPO vector, and expressed in BL21(DE3)Star cells (Life Technologies Japan Inc., Tokyo, Japan). The recombinant proteins were purified using His•Bind® Resin (Merck KGaA, Darmstadt, Germany) and used for raising antisera in rabbits or mice. Immunization of animals and collection of antisera were in part carried out by Medical & Biological Laboratories Co., Ltd., Nagoya, Japan. All animal experiments were carried out in accordance with the fundamental guidelines for animal experiments under the jurisdiction of the Ministry of Education, Culture, Sports, Science and Technology (Notice No. 71, 2006), and approved by the Committee for Animal Experimentation of Juntendo University with the Approval No. 270081.

(c) Western blots

20 μg of protein from the cell supernatant were separated onto a SuperSep® Ace 10-20 % gel (Wako Pure Chemical Industries, Ltd., Osaka, Japan) and transferred to a polyvinylidene fluoride membrane under semi-dry conditions at 20 V for 30 minutes. After blocking with 5% fetal bovine serum (FBS) in phosphate-buffered saline containing 0.25 % tween20 (PBST), the membranes were incubated overnight at 4°C with the antisera to each glycolytic enzyme in 1% FBS/PBST, washed with PBST, and incubated with HRP-conjugated secondary antibody (Jackson ImmunoResearch Laboratories Inc., PA), followed by chemiluminescent development. The reaction was visualized using ImageQuant LAS-4000 min (GE Healthcare Japan Inc., Tokyo, Japan).

(d) Electron microscopy

Cells of the late-log phase were harvested, washed twice in artificial marine water, and fixed as described [13]. Ultrathin sections were stained with lead citrate and uranyl acetate and examined with a transmission electron microscope at 75 kV (Hitachi H-7100, Hitachi High-Technologies Co. Ltd., Tokyo, Japan). For immunoelectron microscopy, cells were fixed using 4% paraformaldehyde and 1% glutaraldehyde in PBS at 4ºC for 2 hrs, dehydrated with ethanol, and embedded in LRWhite at -20ºC for 4 days under UV-light. Ultrathin sections were incubated with 50 mM NH_4Cl in PBS for 2 hours, blocked with 3% BSA in PBS/0.025 % tween20 for 1 hr, and incubated with antisera to *D. papillatum* FBPA [12] for 1 hr. Cells were then incubated with gold-labeled anti-mouse antibody (10 nm particle, Sigma-Aldrich Co. LLC., MO), counterstained with uranyl acetate, and observed using Hitachi H-7100.

(e) Metabolic labeling

The mid-log phase of cells were starved in artificial seawater for 2 hrs and then incubated with 6 mM $^{13}C_6$ D-glucose or 6 mM $^{13}C_5$ L-glutamine (Sigma-Aldrich) in artificial seawater for 0, 4, and 8 hrs or with 30 mM $^{13}C_6$ D-glucose in normal culture medium for 72 hrs without starvation. Cells in the mid-log phase of growth were starved in artificial seawater for 2 hrs and then incubated with 6 mM $^{13}C_6$ D-glucose or 6 mM $^{13}C_5$ L-glutamine (Sigma-Aldrich) in artificial seawater for 0, 4, and 8 hrs or with 30 mM $^{13}C_6$ D-glucose in normal culture medium for 72 hrs without starvation. Cells were then washed twice with 10% w/v mannitol and treated with methanol by vortexing for 1 min. After removing the debris by centrifugation, the supernatant was extracted with 1:0.4 of chloroform and milli-Q water by vortexing for 1 min. The aqueous phase was filtered through an Ultrafree MC PHLCC HMT filter (Merck KGaA, Darmstadt, Germany) having a cut-off of 5 kDa at 9,400 x *g* for 2 hrs to remove proteins. The eluate

containing the metabolites was evaporated and dissolved in 0.05 ml of Milli-Q water. CE-Q-TOFMS analysis was performed using an Agilent CE system combined with a Q-TOFMS (Agilent Technologies, Palo Alto, CA, USA) as described [14-16]. The data obtained by CE-Q-TOFMS analysis were preprocessed using MassHunter workstation software Qualitative Analysis Version B.06.00. Each metabolite was identified and quantified based on the peak information including m/z, migration time, and peak area. The quantified data were then evaluated for statistical significance by a Wilcoxon signed-rank test. Alternatively, liquid chromatography-coupled mass spectrometry (LC-MS) was performed on a TSQ Quantum Ultra AM with the analysis software Xcalibur 2.0.6 software (Thermo Fisher Scientific, San Jose, CA) coupled to a Gilson-HPLC system and a Gilson 234 autosampler (Gilson Inc., WI) as described [17].

(f) Metabolome analysis

Metabolome measurements were carried by Human Metabolome Technology Inc., Tsuruoka, Japan. Briefly, cells were collected in mid-log phase, washed twice with 10% mannitol, and resuspended in methanol containing internal standards (H3304-1002, Human Metabolome Technologies, Inc., Tsuruoka, Japan) followed by ultrasonication, to inactivate enzymes. The metabolites were further extracted and finally dissolved in 50 μL of Milli-Q water for CE-MS analysis.

References

1 Fujii S & Beutler E. 1985 High glucose concentrations partially release hexokinase from inhibition by glucose 6-phosphate. *Proc. Natl. Acad. Sci. USA* **82**, 1552-1554.

2 Misset O & Opperdoes FR. 1984 Simultaneous purification of hexokinase, class-I fructose-bisphosphate aldolase, triosephosphate isomerase and phosphoglycerate kinase from *Trypanosoma brucei*. *Eur. J. Biochem.* **144**, 475-483.

3 Sooranna SR & Saggerson ED. 1982 Rapid modulation of adipocyte phosphofructokinase activity by noradrenaline and insulin. *Biochem. J.* **202**, 753-758.

4 Galkin A, Kulakova L, Melamud E, Li L, Wu C, Mariano P, Dunaway-Mariano D, Nash TE & Herzberg O. 2007 Characterization, kinetics, and crystal structures of fructose-1,6-bisphosphate aldolase from the human parasite, *Giardia lamblia*. *J. Biol. Chem.* **282**, 4859-4867.

5 Molina y Vedia L, McDonald B, Reep B, Brüne B, Di Silvio M, Billiar TR & Lapetina EG. 1992 Nitric oxide-induced S-nitrosylation of glyceraldehyde-3-phosphate dehydrogenase inhibits enzymatic activity and increases endogenous ADP-ribosylation. *J. Biol. Chem.* **267**, 24929-24932.

6 Opperdoes FR & Borst P. 1977 Localization of nine glycolytic enzymes in a microbody-like organelle in *Trypanosoma brucei*: the glycosome. *FEBS Lett.* **80**, 360-364.

7 Yu JS & Noll KM. 1995 The hyperthermophilic bacterium *Thermotoga neapolitana* possesses two isozymes of the 3-phosphoglycerate kinase/triosephosphate isomerase fusion protein. *FEMS Microbiol. Lett.* **131**, 307-312.

8 Chevalier N, Rigden DJ, Van Roy J, Opperdoes FR & Michels PA. 2000 *Trypanosoma brucei* contains a 2,3-bisphosphoglycerate independent phosphoglycerate mutase. *Eur. J. Biochem.* **267**, 1464-1472.

9 Hannaert V, Albert MA, Rigden DJ, da Silva Giotto MT, Thiemann O, Garratt RC, Van Roy J, Opperdoes FR & Michels PA. 2003 Kinetic characterization, structure modelling

studies and crystallization of *Trypanosoma brucei* enolase. *Eur. J. Biochem.* **270**, 3205-3213.

10 Callens M, Kuntz DA & Opperdoes FR. 1991 Characterization of pyruvate kinase of *Trypanosoma brucei* and its role in the regulation of carbohydrate metabolism. *Mol. Biochem. Parasitol.* **47**, 19-29.

11 Misek DE & Saltiel AR. 1992 An inositol phosphate glycan derived from a *Trypanosoma brucei* glycosyl-phosphatidylinositol mimics some of the metabolic actions of insulin. *J. Biol. Chem.* **267**, 16266-16273.

12 Makiuchi T, Annoura T, Hashimoto M, Hashimoto T, Aoki T & Nara T. 2011 Compartmentalization of a glycolytic enzyme in *Diplonema*, a non-kinetoplastid euglenozoan. *Protist* **162**, 482-489. (doi:10.1016/j.protis.2010.11.003).

13 Marande W, Lukeš J & Burger G. 2005 Unique mitochondrial genome structure in diplonemids, the sister group of kinetoplastids. *Eukaryot. Cell* **4**, 1137-1146.

14 Kami K, Fujimori T, Sato H, Sato M, Yamamoto H, Ohashi Y, Sugiyama N, Ishihama Y, Onozuka H, Ochiai A, et al. 2013 Metabolomic profiling of lung and prostate tumor tissues by capillary electrophoresis time-of-flight mass spectrometry. *Metabolomics* **9**, 444-453. (doi:10.1007/s11306-012-0452-2).

15 Ohashi Y, Hirayama A, Ishikawa T, Nakamura S, Shimizu K, Ueno Y, Tomita M & Soga T. 2008 Depiction of metabolome changes in histidine-starved *Escherichia coli* by CE-TOFMS. *Mol. Biosyst.* **4**, 135-147. (doi:10.1039/b714176a).

16 Ooga T, Sato H, Nagashima A, Sasaki K, Tomita M, Soga T & Ohashi Y. 2011 Metabolomic anatomy of an animal model revealing homeostatic imbalances in dyslipidaemia. *Mol. Biosyst.* **7**, 1217-1223. (doi:10.1039/c0mb00141d).

17 Olszewski KL, Mather MW, Morrisey JM, Garcia BA, Vaidya AB, Rabinowitz JD & Llinas M. 2010 Branched tricarboxylic acid metabolism in *Plasmodium falciparum*. *Nature* **466**, 774-778. (doi:10.1038/nature09301).

Table S1. Predicted PTS in non-glycolytic enzymes of *Diplonema papillatum*.

Enzyme	PTS*	
	D. papillatum	***T. brucei***
Gluconeogenesis		
Malate dehydrogenase (MDH), glycosomal	ND	PTS1
Phosphoenolpyruvate carboxykinase (PEPCK)	ND	PTS1
Pentose phosphate pathway		
6-phosphogluconolactonase	ND	PTS1
Ribokinase	ND	PTS1
Transketolase	ND	PTS1
Energy/redox metabolism		
Adenylate kinase	ND	PTS1
Glycerol 3-phosphate dehydrogenase	ND	PTS1
Glycerol kinase (GK)	PTS1	PTS1
Isocitrate dehydrogenase	ND	PTS1
NADH-dependent fumarate reductase	ND	PTS1
Pyruvate phosphate dikinase (PPDK)	PTS1	PTS1
Pyrimidine biosynthesis/purine salvage		
Adenine phosphoribosyltransferase	ND	PTS1
Guanylate kinase	ND	PTS1
Hypoxanthine-guanine phosphoribosyltransferase	ND	PTS1
Inosine-5'-monophosphate dehydrogenase	ND	PTS1
Orotate phosphoribosyltransferase (OPRT)	ND	PTS1†
Orotidine monophosphate decarboxylase (OMPDC)	ND	PTS1†

*PTS1 represents being double positive for both the C-terminal consensus tripeptides, (STAGCN)-(RKH)-(LIVMAFY), and a category of “targeted” or “twilight zone” using the PTS1 predictor (see materials and methods).
†Fused in OMPDC-OPRT.
ND; No PTS detected.

Table S2. Metabolites of carbon metabolism in *Diplonema papillatum*.

Metabolites (pmole/10^8 cells)	*T. cruzi*	*D. papillatum*[a]	*D. papillatum*[b]	*D. papillatum*[c]
Glycolysis				
Hexose phosphate group				
Glucose 6-phosphate	161	21,166	37,182	6,168
Glucose 1-phosphate	77	4,393	5,773	1,435
Fructose 6-phosphate	348	7,895	13,324	2,739
Fructose 1,6-bisphosphate	158	3,490	2,203	769
Triose phosphate group				
Dihydroxyacetone phosphate	129	11,779	5,944	2,600
Glyceraldehyde 3-phosphate	ND	186	ND	ND
3-Phosphoglyceric acid	1,707	4,080	4,442	1,003
2-Phosphoglyceric acid	267	638	777	189
Phosphoenolpyruvic acid	1,036	564	903	ND
Ratio of total hexose-P:triose-P	**744:3149 (1:4.2)**	**36944:17247 (2.1:1)**	**58482:12066 (4.8:1)**	**11111:3792 (2.9:1)**
TCA cycle				
Citric acid	330	1,705	894	401
cis-aconitic acid	ND	924	532	237
Isocitric acid	ND	70,382	53,107	21,083
α-ketoglutaric acid	ND	4,397	4,412	3,180
Succinic acid	35,203	108,395	113,315	22,092
Fumaric acid	126	6,454	2,204	1,492
Malic acid	535	22,612	15,545	9,739
Pentose phosphate pathway				
6-Phosphogluconic acid	21	73	ND	ND
Ribulose 5-phosphate	144	1,859	1,906	511
Ribose 5-phosphate	38	585	638	128
Sedoheptulose 7-phosphate	282	1,729	5,199	443
Erythrose 4-phosphate	ND	572	353	ND
Nucleotides				
ATP	8,578	6,944	9,481	1,247
ADP	8,010	19,800	19,395	6,637
AMP	8,028	50,665	23,739	14,455
cAMP	15	ND	ND	ND
GTP	2,264	1,228	2,116	607
GDP	2,196	4,572	4,143	2,223
GMP	1,208	6,643	3,884	3,248
UTP	4,974	1,984	2,259	290
UDP	5,083	4,847	4,626	1,502
UMP	5,571	11,936	5,445	2,657
CTP	583	139	400	ND
CDP	360	302	528	280
CMP	457	2,560	2,407	1,424

[a] ATCC® 1405 artificial seawater supplemented with 10 % v/v horse serum.
[b] ATCC® 1532 medium.
[c] ATCC® 1532 medium supplemented with 6 mM D-glucose.
ND, not detected.

Table S2. *Continued.*

Metabolites (pmole/10^8 cells)	*T. cruzi*	*D. papillatum*[a]	*D. papillatum*[b]	*D. papillatum*[c]
Others				
Pyruvic acid	126	1,372	2,351	1,820
Lactic acid	11,800	82,962	84,245	20,330
Amino acids				
β-Ala	147	1,191,232		
Glu	14,748	842,686		
Lys	20,288	453,660		
Pro	17,256	423,095		
Ala	212,561	367,248		
Gln	86	317,801		
Arg	11,335	217,878		
Gly	99,373	137,363		
Val	36,898	134,090		
His	200	109,362		
Ser	507	98,449		
Thr	338	85,611		
Leu	3,968	78,799		
Tyr	929	73,437		
Asn	1,700	53,480		
Asp	1,578	51,883		
Ile	15,529	35,984		
Phe	808	35,481		
Trp	290	15,796		
Met	244	12,534		
Cys	ND	569		

[a] ATCC® 1405 artificial seawater supplemented with 10 % v/v horse serum.
[b] ATCC® 1532 medium.
[c] ATCC® 1532 medium supplemented with 6 mM D-glucose.
ND, not detected.

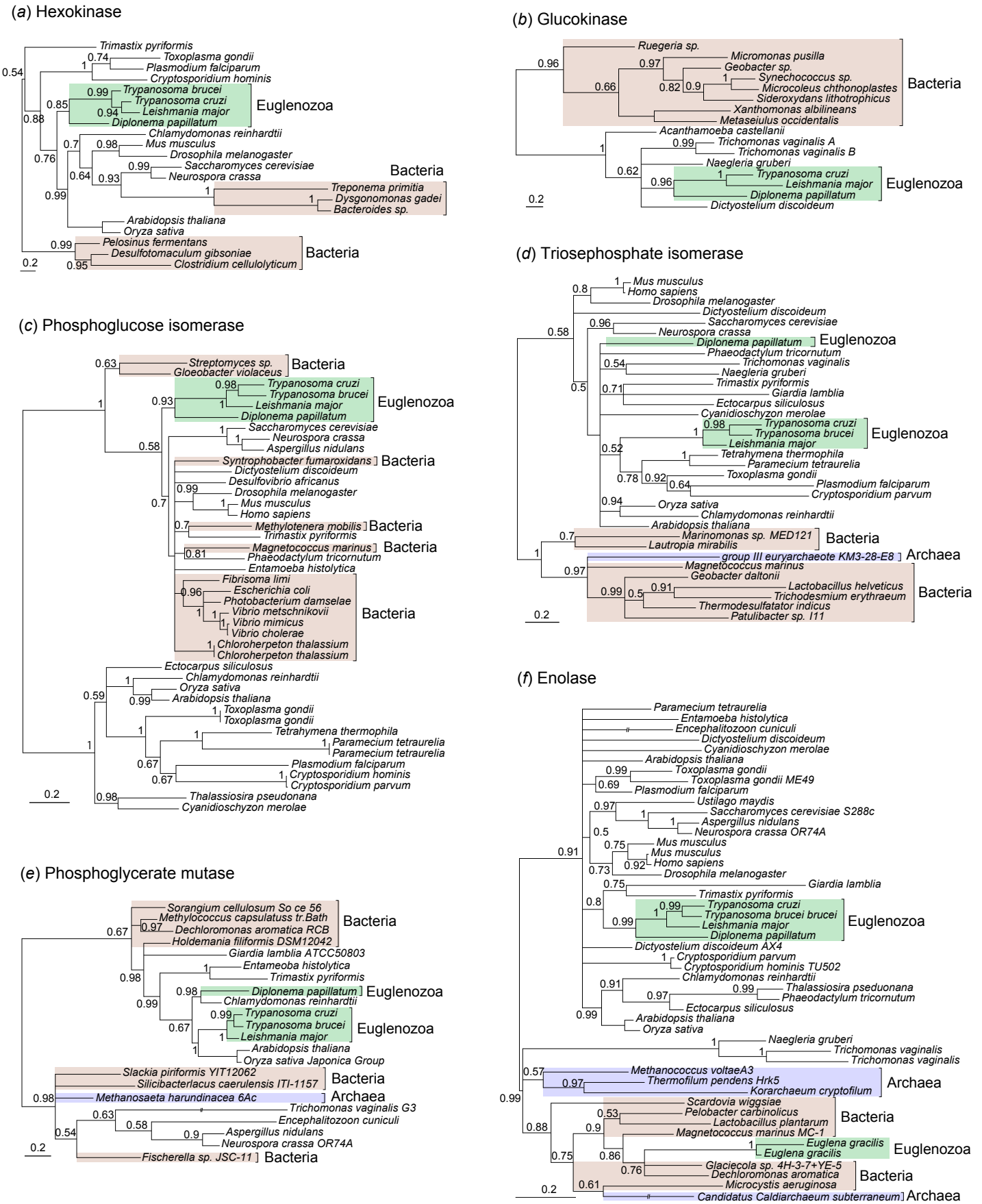

Figure S1. Consensus phylogenetic trees for glycolytic enzymes. (*a*) Hexokinase; (*b*) glucokinase; (*c*) phophoglucose isomerase; (*d*) triose phosphate isomerase; (*e*) phophoglycerate mutase; and (*f*) enolase. Euglenozoa, bacteria and archaea are labeled in green, brown, and gray, respectively. The detailed methods to reconstruct the phylogenetic trees are described in the materials and methods.

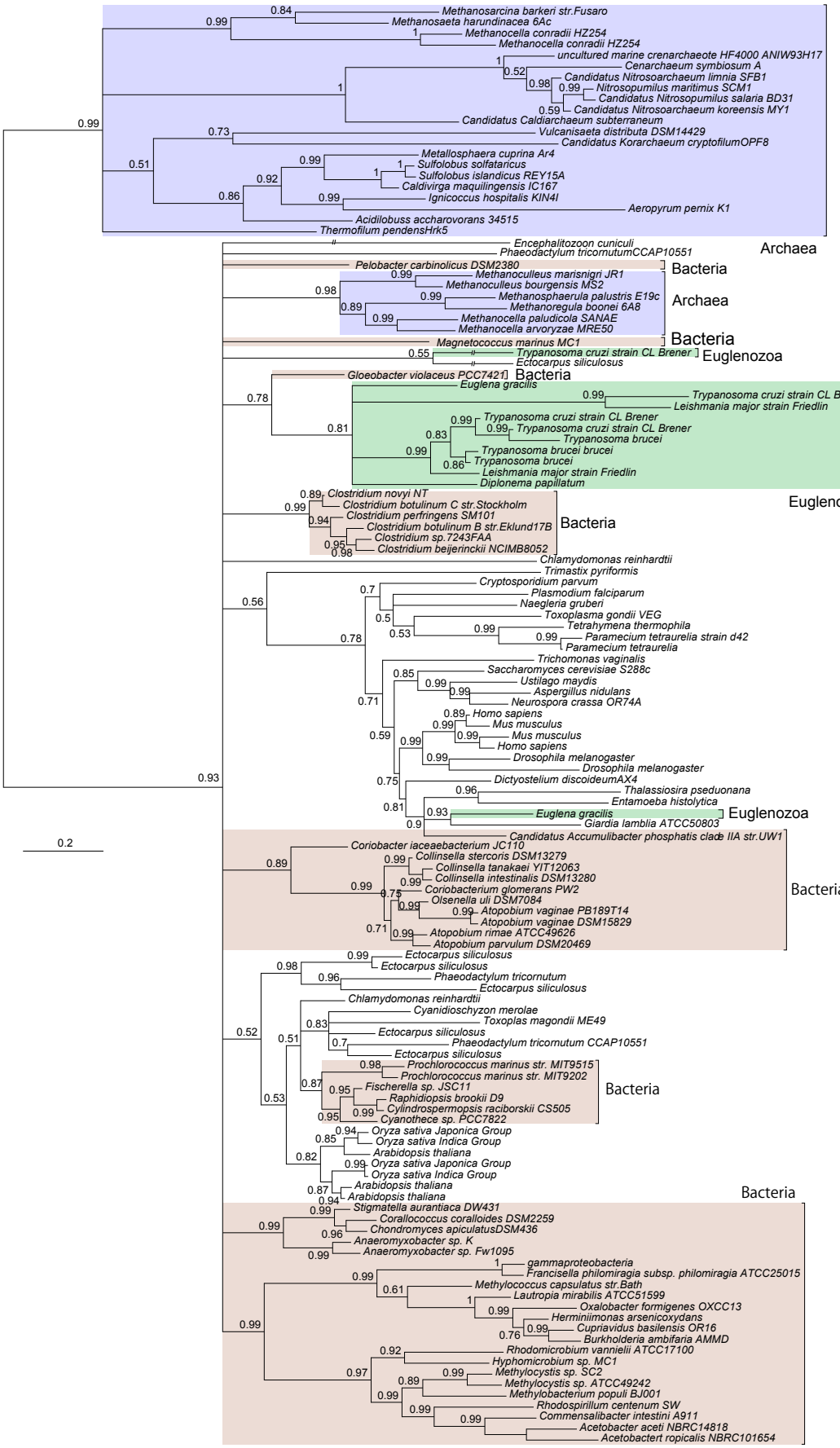

Figure S2. Consensus phylogenetic tree for phosphoglycerate kinase. The methods and labeling are as in figure S1.

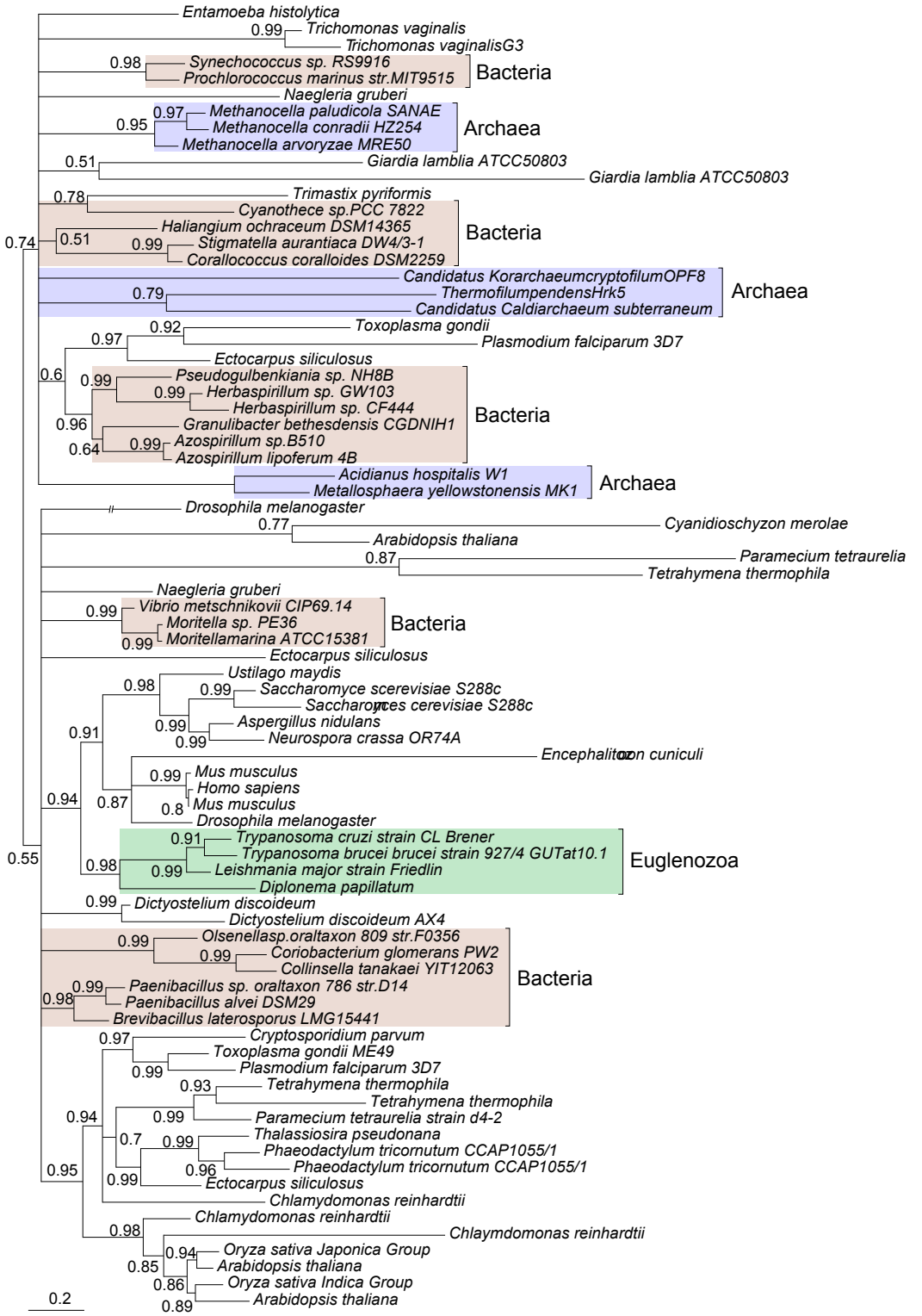

Figure S3. Consensus phylogenetic tree for pyruvate kinase. The methods and labeling are as in figure S1.

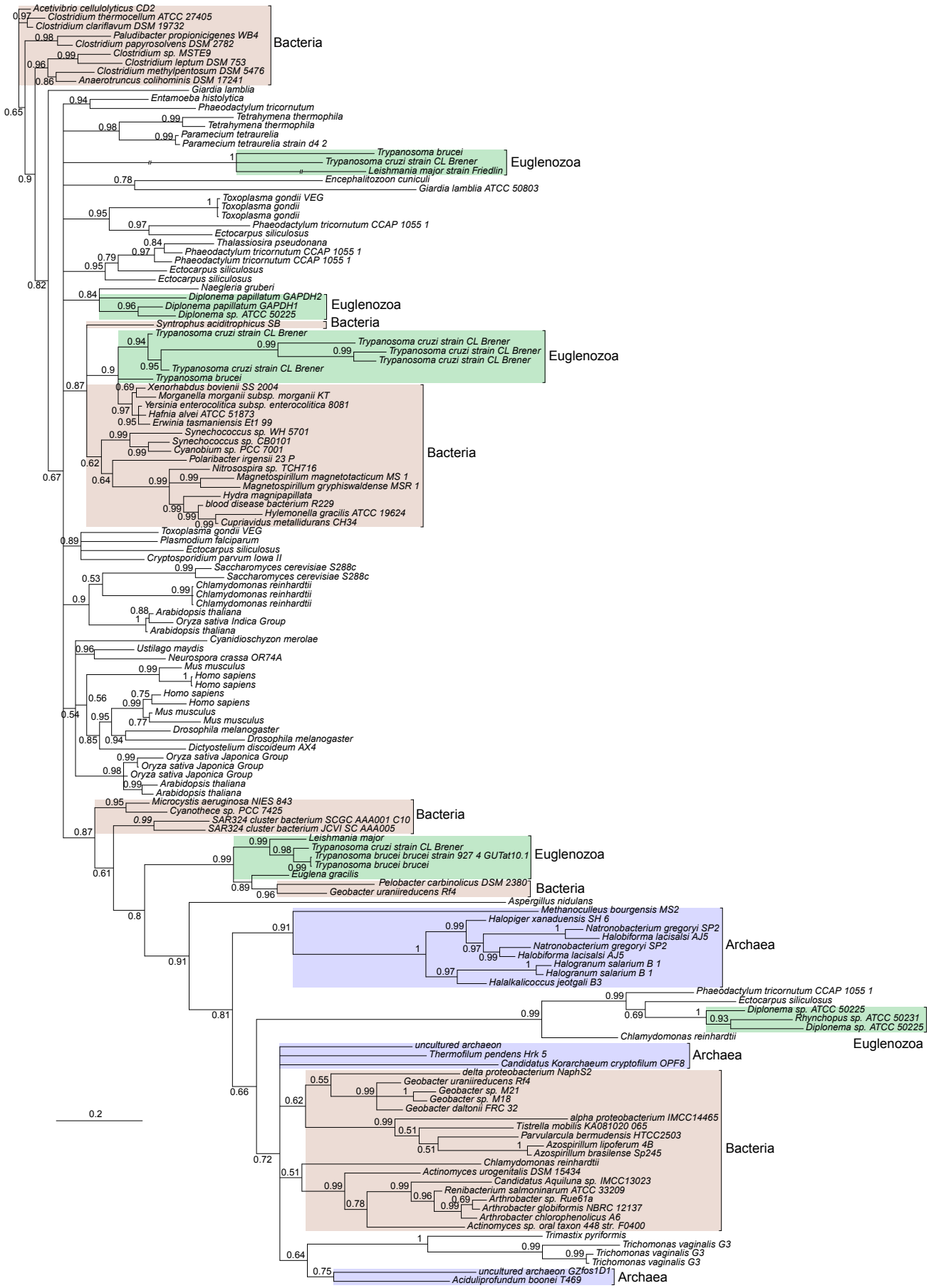

Figure S4. Consensus phylogenetic tree for glyceraldehyde-3-phosphate dehydrogenase. The methods and labeling are as in figure S1.

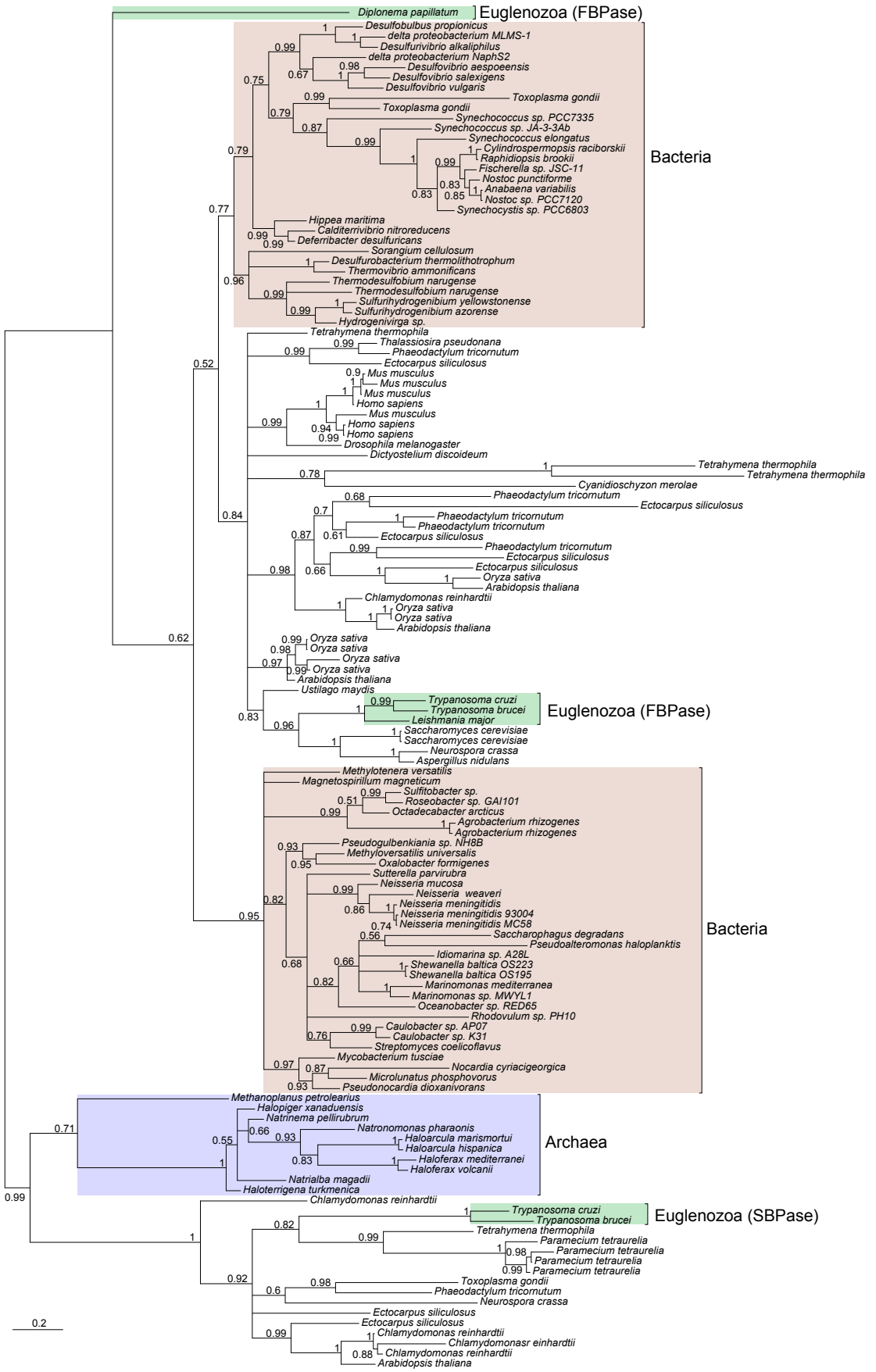

Figure S5. Consensus phylogenetic tree for fructose-1,6-bisphosphatase (FBPase). Sedoheptulose-1,7-bisphosphatase (SBPase) is an enzyme for pentose phosphate pathway. The methods and labeling are as in figure S1.

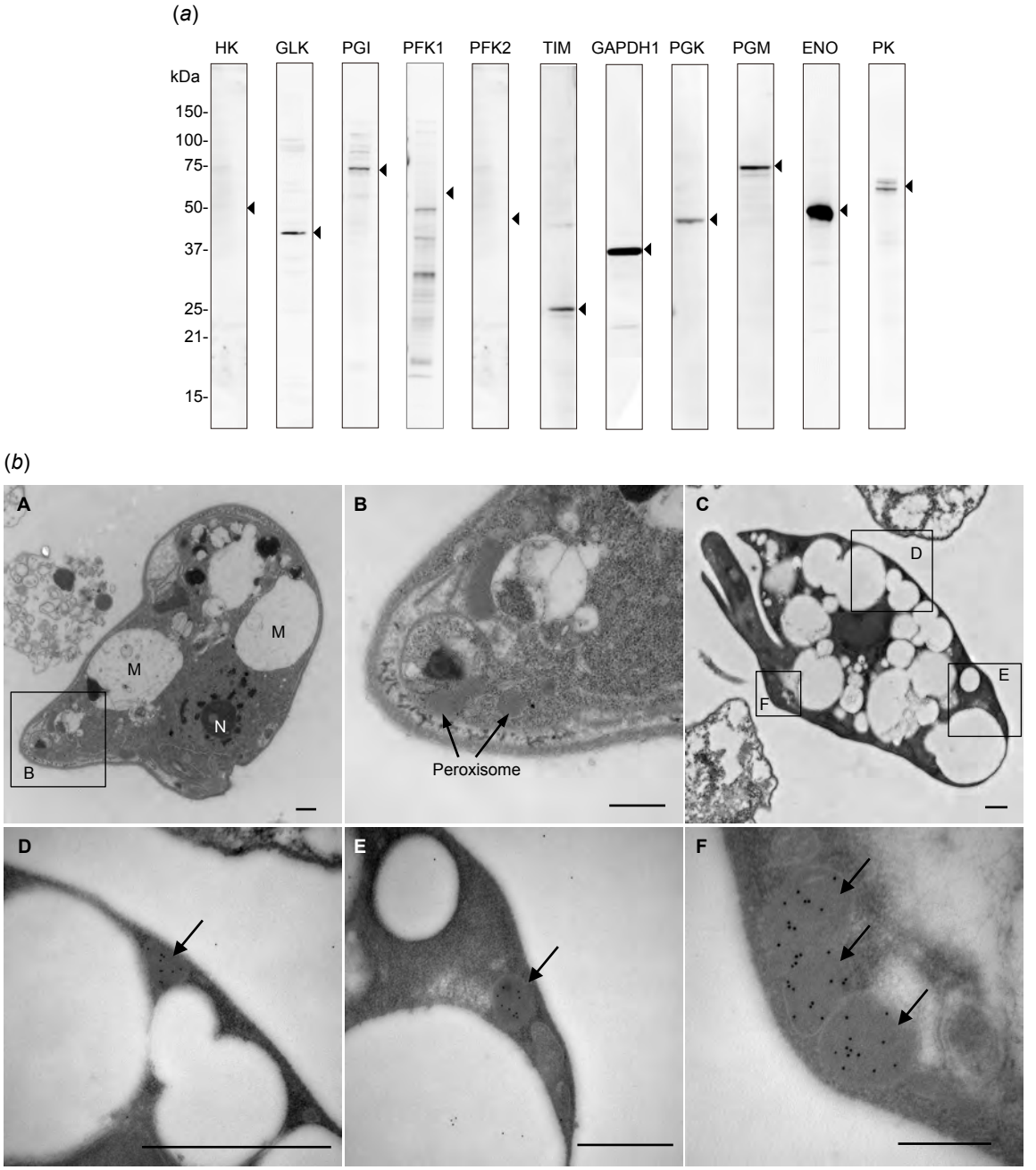

Figure S6. Expression of glycolytic enzymes in *D. papillatum*. (*a*) Western blot analysis of the *D. papillatum* extracts using antisera to the relevant enzymes. The expected size of each protein is shown by a triangle in each panel. (*b*) Ultrastructure of *D. papillatum*. Peroxisomes (arrow) are present as dense bodies surrounded by a single-membrane (B, a magnified image of the inset of A). C-F, Immunoelectron microscopic observations of FBPA within peroxisomes. Note that gold particles are specifically detected inside peroxisomes (arrow). (D, E, and F are magnified images of the insets of C). N; nucleus. M; mitochondrion, P; peroxisome. Scale bar = 0.5 μm.

(*a*) 6 mM $^{13}C_5$-L-glutamine

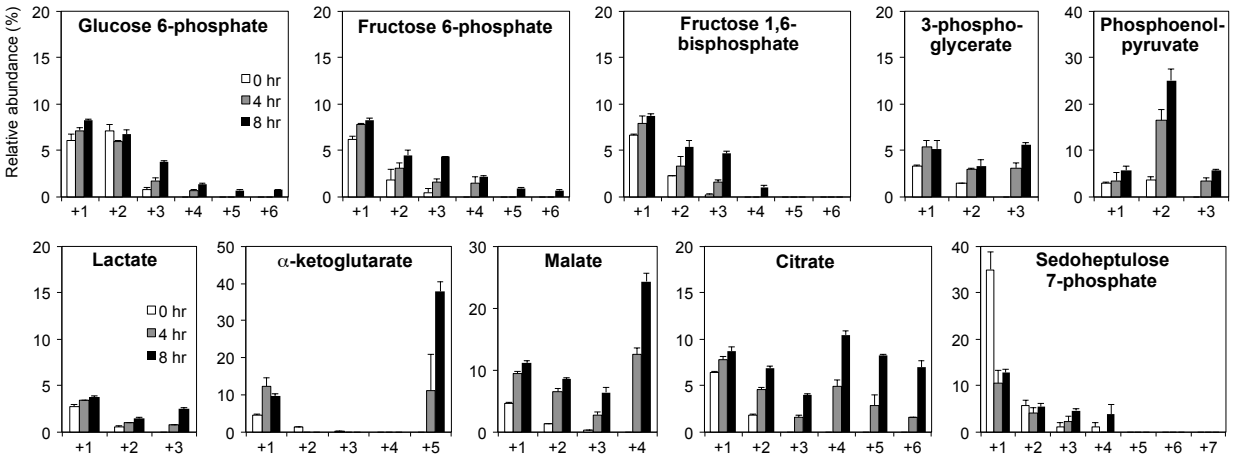

(*b*) 6 mM $^{13}C_6$-D-glucose

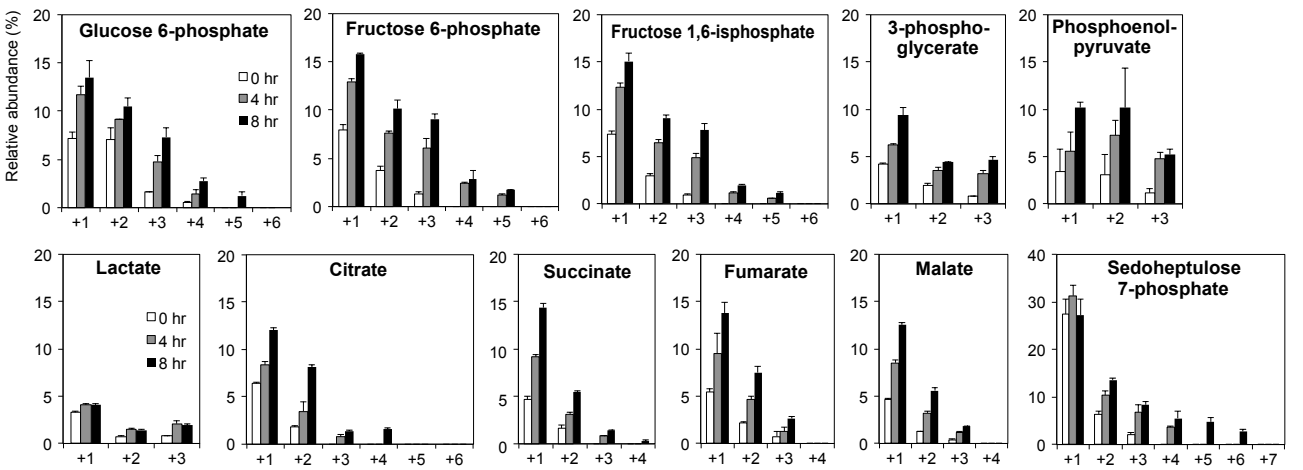

(*c*) 30 mM $^{13}C_6$-D-glucose

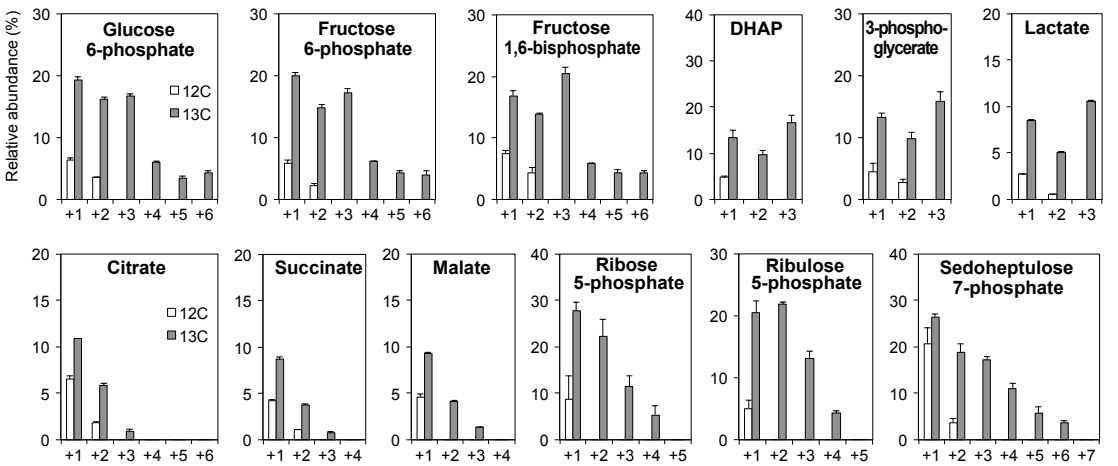

Figure S7. Metabolomic analysis of ^{13}C-labeled metabolites in *D. papillatum*. *D. papillatum* cells were incubated with 6 mM $^{13}C_5$-glutamine for 0, 4, and 8 hrs (*a*), 6 mM $^{13}C_6$-D-glucose for 0, 4, and 8 hrs (*b*), or 30 mM $^{13}C_6$-D-glucose for 72 hrs (*c*). The Y-axis indicates the relative abundance (%) of each isotopomer of the relevant metabolite. The X-axis represents the number of ^{13}C in the isotopomers. Data points and error bars represent the mean ± s.d. of three independent experiments.

Figure S8. Consensus phylogenetic tree for adenylate kinase. Note that *E. gracilis* enzyme and the glycosomal enzymes of kinetoplastids are nested independently within the bacterial clade (PP = 0.99), while *D. papillatum* and cytosolic kinetoplastid homologues cluster in the eukaryotic subtree (PP = 0.99). The methods and labeling are as in figure S1.

Figure S9. Consensus phylogenetic tree for inosine-5-monophosphate dehydrogenase. Note that glycosomal isoforms of kinetoplastids are nested within the bacterial clade, while *E. gracilis*, *D. papillatum* and cytosolic kinetoplastid homologues are monophyletic and cluster in the eukaryotic clade, consistent with the organismal tree (PP = 1). The methods and labeling are as in figure S1.

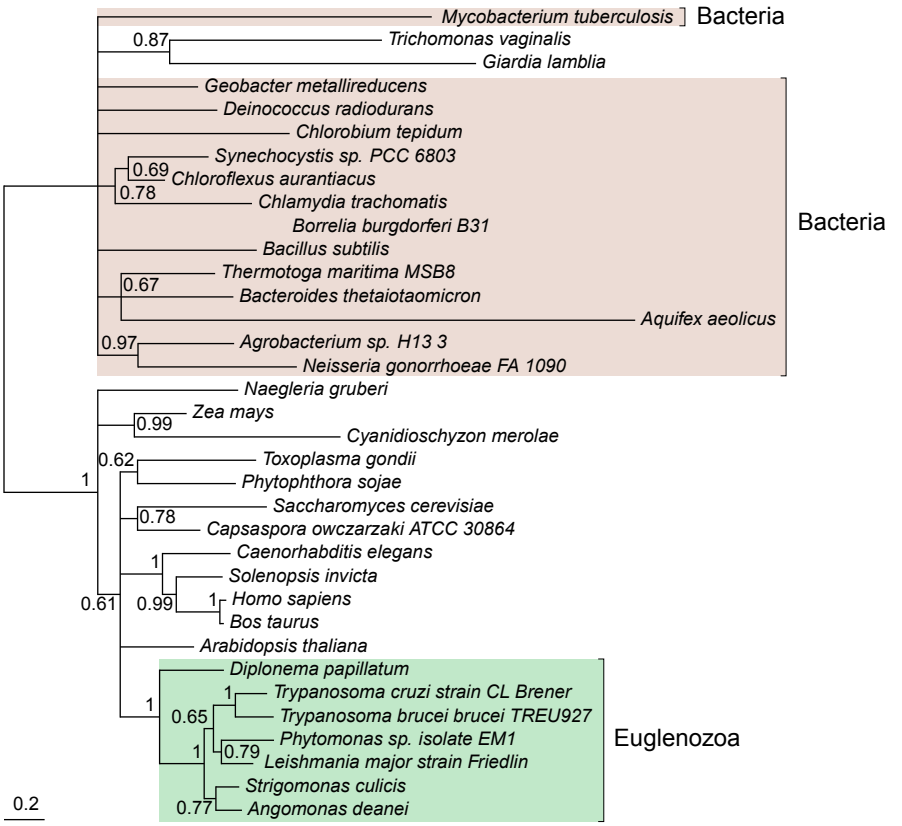

Figure S10. Consensus phylogenetic tree for transketolase. Note that the euglenozoan enzymes are monophyletic (PP = 1). The methods and labeling are as in figure S1.